STUDIA UNIV. "BABEŞ–BOLYAI", MATHEMATICA, Volume **LI**, Number 4, December 2006

LAPLACIAN DECOMPOSITION METHOD FOR INVERSE STOKES PROBLEMS

A.E. CURTEANU, L. ELLIOTT, D.B. INGHAM AND D. LESNIC

Dedicated to Professor Gheorghe Coman at his 70^{th} *anniversary*

Abstract. This paper considers an inverse boundary value problem associated to the Stokes equations which govern the motion of slow viscous incompressible fluid flows. The solution of these equations is analyzed using a novel technique based on a Laplacian decomposition instead of the more traditional approaches based on the biharmonic streamfunction formulation or the velocity-pressure formulation. The determination of the under-specified boundary values of the normal fluid velocity is made possible by utilizing within the analysis additional pressure measurements which are available from elsewhere on the boundary. Results both on the boundary and inside the solution domain are presented and discussed for a simple benchmark test example and an application in a square geometry in order to illustrate that the Laplacian decomposition in combination with BEM provides an efficient technique, in terms of accuracy, convergence and stability to investigate numerically an inverse Stokes flow.

1. Introduction

Due to the mathematical complexity of the Navier-Stokes equations, it is well known that the general solution of these equations is not possible. Therefore in order to construct tractable mathematical models of the fluid flow systems, it is necessary to resort to a number of simplifications. One of these simplifications occurs when viscous forces are of a higher-order in magnitude as compared to the inertial

Received by the editors: 20.06.2006.

2000 *Mathematics Subject Classification.* 76D07,35J05, 34A55, 74S15.

Key words and phrases. Laplacian decomposition, inverse problems, Stokes flow, boundary element method.

forces. Consequently, one may drop the inertia terms from the steady Navier-Stokes equations to obtain:

$$\mu\overline{\nabla}^2\ \underline{\overline{q}} = \overline{\nabla}\ \overline{P} \tag{1}$$

where $\underline{\overline{q}}$ is the fluid velocity vector, $\overline{P}$ the pressure, ρ the density and μ the fluid viscosity. Equation (1) is called the steady Stokes equation and may be regarded as the fundamental equation for the very slow motion of viscous fluids, known as creeping flows or Stokes flows. Non-dimensionalising equation (1), using typical velocity and length scales U_0 and L, respectively, and defining $\underline{\overline{r}} = L\underline{r}$, $\underline{\overline{q}} = \overline{U_0}\underline{q}$ and $\overline{P} = \frac{\mu\overline{U_0}}{L}P$, results in

$$\nabla^2\ \underline{q} = \nabla\ P. \tag{2}$$

Since the fluid flow is assumed to be incompressible, we also have the continuity equation

$$\nabla \cdot \underline{q} = 0. \tag{3}$$

If exact data for u and v are specified at all the points on the boundary $\partial\Omega$ then the velocity and the pressure can be determined everywhere inside the solution domain Ω. However, in many practical situations it is not always possible to specify both components of the velocity at all the points on the boundary. Consequently, a part of the boundary remains under-specified and in order to compensate for this under-specification extra information is used on another part of the boundary, which gives rise to a portion of the boundary being over-specified. Such problems are called inverse problems and as Hadamard [4] pointed out their solution may not depend continuously on the input data.

In practical problems the additional information has to come from measurements and frequently it is easier to measure the pressure, in addition to the fluid velocity, rather than the vorticity. Therefore, in this paper we introduce extra information on pressure and, clearly, in this case it is more appropriate to work with the Stokes equations rather than the biharmonic equation. Nevertheless, the initial step

in obtaining a numerical solution of such an inverse and ill-posed problem is to develop a method of solution for the corresponding direct problem. The velocity-pressure formulation for direct Stokes problems, based on the Laplacian decomposition and BEM, has been described elsewhere, for example, in Curteanu *et al.* [3].

In the underlying inverse Stokes problem, we investigate the numerical solution in a domain Ω enclosed by a non-smooth boundary $\partial\Omega$, such that

$$\partial\Omega = \Gamma \cup \Gamma_0 \tag{4}$$

where Γ_0 is the under-specified boundary section and $\Gamma = \partial\Omega - \Gamma_0$. Both the normal and the tangential components of the fluid velocity, namely u and v are specified on the section of the boundary Γ, whilst only the tangential component is given on Γ_0. However, this under-specification of the boundary conditions on Γ_0 is compensated by the additional pressure measurements over $\Gamma^* \subseteq \Gamma$. This problem has been previously solved by Zeb *et al.* [8] where they used the BEM on the full Stokes equations.

Furthermore, the system of algebraic equations that results from an application of the BEM, in conjunction with the boundary conditions, is solved using the zeroth-order Tikhonov regularization method. The numerical solutions are obtained for the unspecified values of both the normal component of the fluid velocity and of the boundary pressure. Due to the ill-posed nature of the inverse Stokes problems described above, it is important to consider the stability of the numerical solution. Therefore we investigate the effect of noise on the numerical solution for the unknown values of the normal fluid velocity and the boundary pressure by adding a random error to the input data. Perturbation in the tangential component has not been considered, because, in general, this information is physically available from the no-slip condition on the solid boundary and is unlikely to contain any noise.

2. **Mathematical formulation**

For what follows, it is not restrictive to assume two-dimensional flows in a bounded domain $\Omega \subseteq \mathbb{R}^2$. Differentiating the x and y components of equation (2) with respect to x and y, respectively, then adding together and using the continuity

equation, results in

$$\nabla^2 P = 0. \tag{5}$$

In order to simplify equations (2) and (3), the following formulation for the velocity $\underline{q} = (u, v)$ components are introduced:

$$u = f + \frac{x}{2}P, \tag{6}$$

$$v = g + \frac{y}{2}P. \tag{7}$$

From (2) and (5) this results in f and g being solutions of the Laplace equation, namely

$$\nabla^2 f = 0, \tag{8}$$

$$\nabla^2 g = 0. \tag{9}$$

The above substitutions have reduced the Stokes problem to the solution of three Laplace's equations, (5), (8) and (9), interconnected through some boundary conditions involving also the continuity equation (3).

It is well known that the harmonic function P in equations (6) and (7) is unique up to an arbitrary constant, a. Moreover, if f_0, g_0 and P_0 are harmonic functions subject to the prescribed boundary conditions on u and v, then so are $f_0 - \frac{ax}{2}$, $g_0 - \frac{ay}{2}$ and $P_0 + a$. However, this non-uniqueness can be easily avoided by prescribing the value of the pressure at one arbitrary spatial point and this holds for the inverse problem considered - the pressure being prescribed on a part of the boundary.

BEM - Integral equation

In this paper, the development of the BEM for discretising the Laplace equation is the classical approach, see Brebbia *et al.* [1], and it is based on using the fundamental solution for the Laplace equation and Green's identities. Thus, for example, equation $\nabla^2 f = 0$ may be recast as follows:

$$\eta(X) f(X) = \int_\Gamma \{f'(Y) G(X,Y) - f(Y) G'(X,Y)\} d\Gamma_Y \tag{10}$$

where

(i) $X \in \Omega \cup \Gamma$ and $Y \in \partial\Omega$ and $\partial\Omega$ is the boundary of the domain Ω,

(ii) $d\Gamma_Y$ denotes the differential increment of $\partial\Omega$ at Y,

(iii) $\eta(X) = 1$ if $X \in \Omega$, and $\eta(X) =$ the internal angle between the tangents to $\partial\Omega$ on either side of X divided by 2π if $X \in \partial\Omega$,

(iv) G is the fundamental solution for the Laplace equation which in two-dimensions is given by

$$G(X,Y) = -\frac{1}{2\pi} ln|X - Y| \tag{11}$$

(v) G', f' are the outward normal derivatives of G and f, respectively.

We note that, as with the classical constant BEM, nodal points are situated only at the segment mid-points and therefore f' has precisely one value at each of these nodal points. However, with the linear BEM formulations, nodes are situated at segment end-points and therefore, if the domain has corners, at those points f' has two components, one related to each of the sides adjacent to the corner. Therefore, in order to deal with corners and singularities, discontinuous linear boundary elements are introduced in this section.

In practice, the integral equation (10) can rarely be solved analytically and thus some form of numerical approximation is necessary. Based on the BEM, we subdivide the boundary $\partial\Omega$ into a series of N elements $\partial\Omega_j$, $j = \overline{1,N}$, and approximate the functions f and f' at the collocation points of each boundary element Γ_j. In the discontinuous linear elements method (DLBEM) it is assumed that the variables in the integral equation (10) have a linear evolution along the elements. These boundary elements are segments of a straight line and the linear evolution is expressed through the values of the functions at two internal points given by

$$X^j_{\tau,1} = (1-\tau)X_{j-1} + \tau X_j \tag{12}$$

$$X^j_{\tau,2} = \tau X_{j-1} + (1-\tau)X_j \tag{13}$$

where $\tau \in (0, \frac{1}{2})$. Correspondingly, the boundary integral equation (10) becomes

$$\begin{aligned}
\eta(X)f(X) &= \sum_{j=1}^{N} f'_{2j-1}\left[\frac{1-\tau}{1-2\tau}C_j(X) - \frac{1}{1-2\tau}E_j(X)\right] \\
&+ \sum_{j=1}^{N} f'_{2j}\left[\frac{1}{1-2\tau}E_j(X) - \frac{\tau}{1-2\tau}C_j(X)\right] \\
&- \sum_{j=1}^{N} f_{2j-1}\left[\frac{1-\tau}{1-2\tau}D_j(X) - \frac{1}{1-2\tau}F_j(X)\right] \\
&- \sum_{j=1}^{N} f_{2j}\left[\frac{1}{1-2\tau}F_j(X) - \frac{\tau}{1-2\tau}D_j(X)\right] \qquad (14)
\end{aligned}$$

where C_j, D_j, E_j and F_j have the same meaning as in Mera *et al.* [6] and may be evaluated analytically. In the DLBEM, the discretised boundary integral equation (14) is applied on the boundary at each of the points $X^j_{\tau,1}$, $X^j_{\tau,2}$, $j = \overline{1,N}$, leading to a system of $2N$ equations

$$\sum_{j=1}^{2N}\left(A_{ij}f'_j - B_{ij}f_j = 0\right) \quad \text{for} \quad i = \overline{1,2N} \qquad (15)$$

where the matrices A_{ij} and B_{ij} are given by

$$\begin{aligned}
A_{i,2j-1} &= \frac{1-\tau}{1-2\tau}C_j(\underline{z}_i) - \frac{1}{1-2\tau}E_j(\underline{z}_i) \quad \text{for} \quad i = \overline{1,2N}, \quad j = \overline{1,N} \\
A_{i,2j} &= \frac{1}{1-2\tau}E_j(\underline{z}_i) - \frac{\tau}{1-2\tau}C_j(\underline{z}_i) \quad \text{for} \quad i = \overline{1,2N}, \quad j = \overline{1,N} \\
B_{i,2j-1} &= \frac{1-\tau}{1-2\tau}D_j(\underline{z}_i) - \frac{1}{1-2\tau}F_j(\underline{z}_i) \quad \text{for} \quad i = \overline{1,2N}, \quad j = \overline{1,N} \quad i \neq 2j-1 \\
B_{i,2j} &= \frac{1}{1-2\tau}F_j(\underline{z}_i) - \frac{\tau}{1-2\tau}D_j(\underline{z}_i) \quad \text{for} \quad i = \overline{1,2N}, \quad j = \overline{1,N} \quad i \neq 2j
\end{aligned}$$

and the collocation points $\underline{z}_i$, $i = 1, 2N$ are given by

$$\underline{z}_{2i-1} = X^i_{\tau,1} \quad \underline{z}_{2i} = X^i_{\tau,2} \quad i = \overline{1,N} \qquad (16)$$

Similar equations are obtained for the harmonic functions g and P.

Now the equations (8), (9) and (5) reduce to a system of $6N$ equations in $12N$ unknowns, i.e.

$$\begin{cases} A\boldsymbol{f'} - B\boldsymbol{f} = 0 \\ A\boldsymbol{g'} - B\boldsymbol{g} = 0 \\ A\boldsymbol{P'} - B\boldsymbol{P} = 0 \end{cases} \tag{17}$$

In the inverse formulation of the Stokes problem considered in this paper, both components of the fluid velocity, u and v, are specified on the section of the boundary $\Gamma = \partial\Omega - \Gamma_0$, whilst only the tangential component, e.g. u is given on Γ_0. However, this under-specification of the boundary conditions on Γ_0 is compensated by the additional pressure measurements over Γ^*. Clearly, if the velocity vector is known on $\partial\Omega$ then u' and v' can be obtained analytically by using equations $\frac{\partial u}{\partial n} = \pm\frac{\partial u}{\partial x} = \mp\frac{\partial v}{\partial y}$ and $\frac{\partial v}{\partial n} = \pm\frac{\partial v}{\partial y} = \mp\frac{\partial u}{\partial x}$, respectively. Solving the direct problem with u and v known on $\partial\Omega$, we obtain the pressure P everywhere and, in particular, over Γ^*. This numerically calculated pressure, denoted by $P^{(n)}$ is used in the inverse problem (17) and (18).

Suppose that the number of boundary elements N on $\partial\Omega$ is such that N_0 belongs to Γ_0 and N^* to Γ^*. Dividing the boundary such that $\partial\Omega = \Gamma_1 \cup \Gamma_2 \cup \Gamma_3 \cup \Gamma_4$, where $\Gamma_1 = \{(x,y)| -\frac{1}{2} \le x \le \frac{1}{2}, y = -\frac{1}{2}\}$, $\Gamma_2 = \{(x,y)|x = \frac{1}{2}, -\frac{1}{2} \le y \le \frac{1}{2}\}$, $\Gamma_3 = \{(x,y)| -\frac{1}{2} \le x \le \frac{1}{2}, y = \frac{1}{2}\}$, $\Gamma_4 = \{(x,y)|x = -\frac{1}{2}, -\frac{1}{2} \le y \le \frac{1}{2}\}$, the problem can be described mathematically by (17) and the following boundary conditions:

$$\begin{cases} \boldsymbol{f} + \frac{x}{2}\boldsymbol{P} = \boldsymbol{u}^{(n)} - \frac{x}{2}\boldsymbol{P}^{(n)} & \text{on } \partial\Omega \\ \boldsymbol{g} + \frac{y}{2}\boldsymbol{P} = \boldsymbol{v}^{(n)} - \frac{y}{2}\boldsymbol{P}^{(n)} & \text{on } \Gamma \\ \boldsymbol{f'} + \nu_1\boldsymbol{P} + \frac{x}{2}\boldsymbol{P'} = \boldsymbol{u'}^{(n)} - \nu_1\boldsymbol{P}^{(n)} & \text{on } \Gamma_2 \cup \Gamma_4 \\ \boldsymbol{g'} + \nu_2\boldsymbol{P} + \frac{y}{2}\boldsymbol{P'} = \boldsymbol{v'}^{(n)} - \nu_2\boldsymbol{P}^{(n)} & \text{on } \Gamma_1 \cup \Gamma_3 \end{cases} \tag{18}$$

where the N^* vector $\boldsymbol{P}^{(n)}$ is the given pressure on the over-specified part of the boundary $\Gamma^* \subseteq \Gamma$ and $\frac{x}{2}$, $\frac{y}{2}$, $\nu_1 = \frac{\partial(x/2)}{\partial n}$, $\nu_2 = \frac{\partial(y/2)}{\partial n}$ are the matrices $\delta_{ij}\frac{x_{(j)}}{2}$, $\delta_{ij}\frac{y_{(j)}}{2}$, $\delta_{ij}\nu_{1(j)}$ and $\delta_{ij}\nu_{2(j)}$, respectively .

In a generic form, the system of equations (17) and (18) can be rewritten as

$$\mathbb{A}\boldsymbol{x} = \boldsymbol{b} \tag{19}$$

where $\mathbb{A}$ is a known $(12N - 2N_0) \times (12N - 2N^*)$ matrix which includes the matrices A and B, $\boldsymbol{x}$ is a vector of $12N - 2N^*$ unknowns which includes the $2N$ vectors $\boldsymbol{f}|_{\partial\Omega}$, $\boldsymbol{f'}|_{\partial\Omega}$, $\boldsymbol{g}|_{\partial\Omega}$, $\boldsymbol{g'}|_{\partial\Omega}$ and $\boldsymbol{P'}|_{\partial\Omega}$, and the $2N - 2N^*$ vector $\boldsymbol{P}|_{\partial\Omega - \Gamma^*}$ and $\boldsymbol{b}$ is a vector of $12N - 2N_0$ knowns which includes $\boldsymbol{u}|_{\partial\Omega}$, $\boldsymbol{v}|_{\Gamma}$, $\boldsymbol{P}|_{\Gamma^*}$ and the derivatives of velocity. Then, using the calculated boundary data, interior solutions for the harmonic functions and the velocity can be determined explicitly using the integral equation, i.e. equation (10) for f, see Brebbia *et al.* [1].

Regularization method

The Tikhonov regularization method is an efficient method for solving inverse and ill-posed problems which arise in science and engineering. It modifies the least-squares approach and finds an approximate numerical solution which, in the case of the zero-th order regularization procedure, is given by, see Tikhonov and Arsenin [7],

$$\boldsymbol{x} = (\mathbb{A}^t\mathbb{A} + \lambda\mathbb{I})^{-1}\mathbb{A}^t\boldsymbol{b} \tag{20}$$

where $\mathbb{I}$ is the identity matrix, the superscript ^{t} denotes the transpose of a matrix and λ is the regularization parameter, which controls the degree of smoothing applied to the solution and whose choice may be based on the L-curve method, see Hansen [5]. For the zero-th order regularization procedure we plot on a log-log scale the variation of $||\boldsymbol{x}_\lambda||$ against the fitness measure, namely the residual norm $||\mathbb{A}\boldsymbol{x}_\lambda - \boldsymbol{b}||$ for a wide range of values of $\lambda > 0$. In many applications this graph results in a L-shaped curve and the choice of the optimal regularization parameter $\lambda > 0$ is based on selecting approximately the corner of this L-curve.

3. Numerical results

We investigate the solution of Stokes problem given by equations (2) and (3) in a simple two-dimensional non-smooth geometry, such as the square

$$\Omega = \left\{ (x,y) | -\frac{1}{2} < x < \frac{1}{2}, -\frac{1}{2} < y < \frac{1}{2} \right\}.$$

In order to investigate the convergence and the stability of the solution we consider first the following test example, namely the analytical expressions for the three harmonic functions f, g and P are given by:

$$f^{(an)} = -x^3/6 + y^2/2 + xy + xy^2/2 - x^2/2 \tag{21}$$

$$g^{(an)} = -y^2/2 - 3x^2y/2 + x^2/2 + y^3/2 - xy/2 \tag{22}$$

$$P^{(an)} = x^2 - y^2 + x \tag{23}$$

with the corresponding fluid velocity given by:

$$u^{(an)} = x^3/3 + y^2/2 + xy \tag{24}$$

$$v^{(an)} = -y^2/2 - x^2y + x^2/2 \tag{25}$$

For presenting the numerical results, we choose $\Gamma^* = \Gamma_2$. In order to study the effects of various locations for the under-specified boundary region we choose $\Gamma_0 = \Gamma_1$ and $\Gamma_0 = \Gamma_3$. If $\Gamma_0 = \Gamma_2$ and $\Gamma_0 = \Gamma_4$ are to be chosen then the velocity v has to be specified on Γ_0 instead of u, since on this parts of the boundary v is the tangential component.

Whilst in the direct Stokes problem we observed that the difference between the analytical solution and the numerical results for P using $N = 80$ was less than 1%, in the inverse problem, we found $N = 40$ was sufficiently large for the numerical solution to agree graphically with the corresponding numerical solution from the direct problem.

Figure 1(a) shows the numerical solution for the unspecified values of the normal component of the fluid velocity v over $\Gamma_0 = \Gamma_1$ for $\lambda = 10^{-11}$, together with its analytical value specified in the direct problem. From this figure, it is observed

that the agreement between the numerical solution and the one given in equation (25), which is specified analytically over Γ_0 in the direct problem, is excellent. In Figure 1(b), we present the numerical solution for the boundary pressure P over $\partial\Omega - \Gamma^*$ and the boundary pressure obtained from the direct problem. It can be seen in this figure that the numerical solution generated by the inverse problem agrees very well with the corresponding numerical solution obtained from the direct problem.

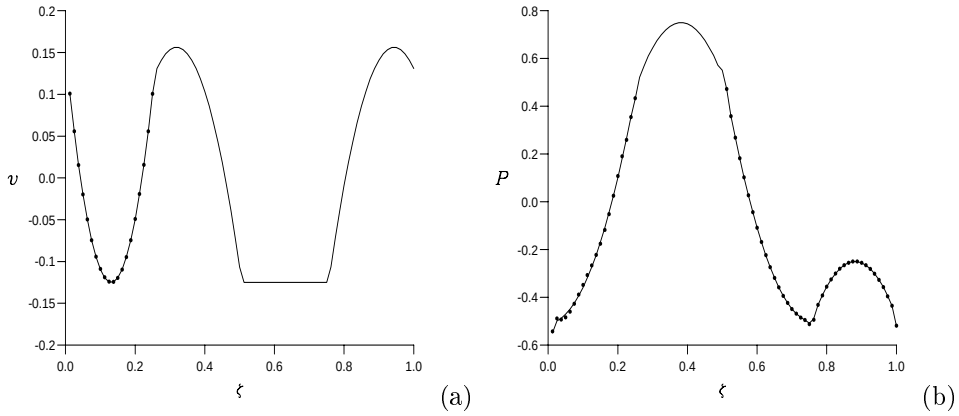

FIGURE 1. The numerical solution (···) for (a) the normal component of the fluid velocity $v|_{\Gamma_0}$, together with the values of v analytically specified over $\partial\Omega$, and (b) the boundary pressure $P|_{\partial\Omega-\Gamma^*}$, together with the corresponding numerical solution for P obtained in the direct problem when $\lambda = 10^{-11}$ using the BEM with 40 discontinuous linear boundary elements.

For various locations of the over-specified boundary region, i.e. $\Gamma^* = \Gamma_3$ or $\Gamma^* = \Gamma_4$, we observed that the numerical results are similar with those obtained for $\Gamma^* = \Gamma_2$. Without presenting the results graphically, we mention that when a different location of the under-specified boundary is chosen, namely $\Gamma_0 = \Gamma_3$ the agreement of the numerical results was found to be equivalent to that observed in Figure 1. Moreover, when we double or more the over-specified part of the boundary,

i.e. $\Gamma^* = \Gamma_2 \cup \Gamma_3$ or $\Gamma^* = \Gamma_2 \cup \Gamma_3 \cup \Gamma_4$, then an even better accuracy is obtained.

Effect of noise

As mentioned in the introduction, the inverse Stokes problem is ill-posed and the system of equations (19) that results is ill-conditioned, and hence the solution may not continuously depend upon the boundary data. Therefore the stability of the regularized boundary element technique is investigated by adding small amounts of noise into the input boundary data in order to simulate measurement errors which are inherently present in the data set of any practical problem. Hence, we perturb the boundary data i.e. data obtained from the direct problem, by adding random noisy perturbations ϵ to the boundary pressure $P^{(n)}$, namely

$$\tilde{P} = P^{(n)} + \epsilon \tag{26}$$

The random error ϵ is generated by using the NAG routine G05DDF, see Brent [2], and it represents a Gaussian random variable with mean zero and standard deviation σ, which is taken to be some percentage α of the maximum value of $P^{(n)}$, i.e.

$$\sigma = \max |P^{(n)}| \times \frac{\alpha}{100} \tag{27}$$

For a particular location of Γ_0, say $\Gamma_0 = \Gamma_1$, Figure 2 shows the L-curve for the inverse problem as a log-log plot of the solution norm $||\boldsymbol{x}_\lambda||$, against the residual norm $||\mathbb{A}\boldsymbol{x}_\lambda - \boldsymbol{b}||$, for various amounts of noise $\alpha = \{3, 6, 10\}$ introduced in $P^{(n)}|_{\Gamma^*}$ and for the various values of the regularization parameter λ taken from the range $[10^{-13}, 10^{-1}]$. We choose the optimal value of the regularization parameter λ, corresponding to the corner of the L-curve, as $\lambda_{opt} = \boldsymbol{O}(10^{-9})$ if $\alpha = 3$ and $\lambda_{opt} = \boldsymbol{O}(10^{-8})$ if $\alpha = \{6, 10\}$.

It was found that the numerical solution for the retrieved normal velocity $v|_{\Gamma_0}$ and pressure $P|_{\partial\Gamma - \Gamma^*}$, obtained using both the exact and noisy data, for λ_{opt} remains stable and agrees with the analytical values and the values specified in the direct problem, respectively, reasonably well according to the amount of noise introduced in the input data for pressure $P|_{\Gamma^*}$. Therefore omitting the boundary results, we present in Figure 3 (a) and (b) the lines of constant pressure and constant velocity

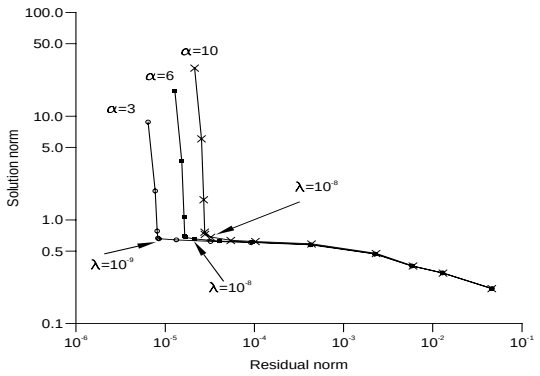

FIGURE 2. The L-curve plot of the solution norm $\| \boldsymbol{x}_\lambda \|$ as a function of the residual norm $\| \mathbb{A}\boldsymbol{x}_\lambda - \boldsymbol{b} \|$ in the inverse Stokes for $N = 40$, $\lambda = [10^{-13}, 10^{-1}]$, when various levels of noise $\alpha = \{3, 6, 10\}$ are added.

component inside the domain Ω and it can be observed that as the amount of noise decreases then the numerical solutions approximate better the solution obtained in the direct problem (for P) or analytically (for v) whilst at the same time remaining stable.

4. **Application - driven cavity**

Now we investigate an inverse problem in a square cavity filled with incompressible viscous fluid and the top lid moving with a constant velocity of unity, for which no analytical solution is available. Now, the tangential component of the fluid velocity is specified on the whole boundary, while the normal component of the fluid velocity v is unknown on e.g. the bottom side of the cavity, namely on $\Gamma_0 = \Gamma_1$ and this under-specification of the boundary conditions is compensated for by the additional pressure measurements on another part of the boundary or over the remaining

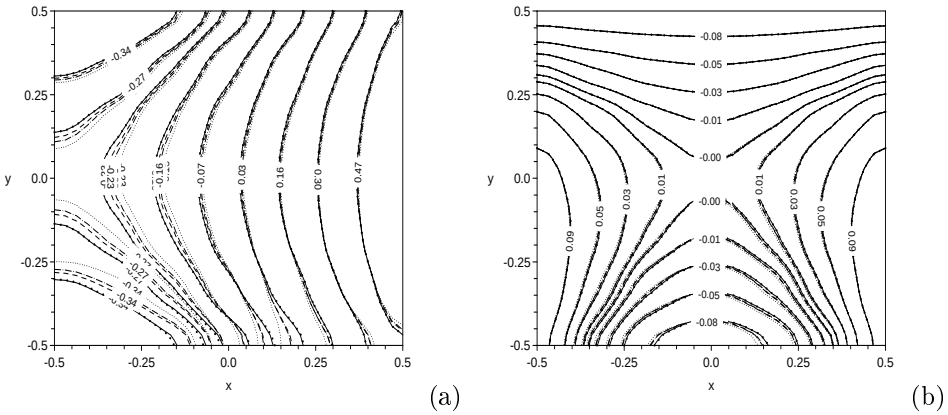

FIGURE 3. The lines of constant (a) pressure P, and (b) velocity v, inside the cavity Ω obtained with $N = 40$ discontinuous linear boundary elements when various levels of noise are introduced in $P|_{\Gamma^*=\Gamma_2}$, namely, (a) direct and (b) analytical solution (——), $\alpha = 0$(• • •), $\alpha = 3$(− − −), $\alpha = 6$(− · − · −·), and $\alpha = 10$(· · ·).

part of the boundary. The boundary conditions for the problem are as follows:

$$\begin{cases} u = v' = 0 & \text{on} \quad \Gamma_0 = \Gamma_1 \\ u = v = u' = 0 & \text{on} \quad \Gamma_2 \\ u = -1, v = v' = 0 & \text{on} \quad \Gamma_3 \\ u = v = u' = 0 & \text{on} \quad \Gamma_4 \\ P = P^{(n)} & \text{on} \quad \Gamma^* \end{cases} \tag{28}$$

When random noise, $\alpha = \{3, 6, 10\}$ is introduced in the pressure $P|_{\Gamma^*}$ the values of the regularization parameter λ given by the L-curve plots, are $\{10^{-10}, 10^{-9}, 10^{-9}\}$ when $\Gamma^* = \Gamma_2$ and $\{10^{-8}, 10^{-7}, 10^{-7}\}$ when $\Gamma^* = \Gamma_2 \cup \Gamma_3 \cup \Gamma_4$. The boundary results were found accurate in comparison with the analytical or direct values and convergent to the exact solutions when the amount of noise decreases. Figure 4 shows the numerical results obtained for pressure inside the driven cavity when different amount of noise are introduced in $P|_{\Gamma^*}$ for two different locations of the over-specified part of the boundary. Also shown in this figure is the corresponding

solution obtained in the direct problem and it is observed that the errors between the numerical solution of the problem (17) and (28) and the values obtained in the direct problem (u and v specified on $\partial\Omega$) are comparable with the amount of noise included and the numerical solution approaches the exact solution with decreasing the amount of noise. Moreover, it can bee seen that the larger is the length of the over-specified part of the boundary, the better is the accuracy.

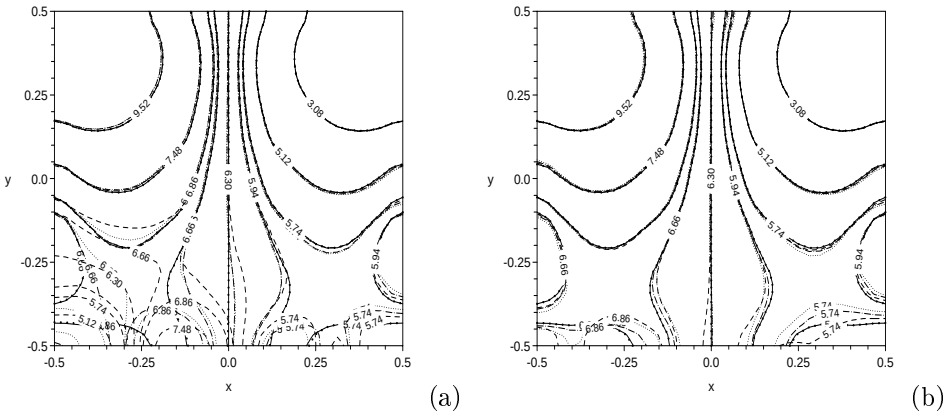

FIGURE 4. The lines of constant pressure P inside the cavity Ω using the BEM with $N = 40$ discontinuous linear boundary elements when various levels of noise are introduced in (a) $P|_{\Gamma^*=\Gamma_2}$ and (b) $P|_{\Gamma^*=\Gamma_2\cup\Gamma_3\cup\Gamma_4}$, namely, direct solution (——), $\alpha = 0$(• • •), $\alpha = 3$(− − −), $\alpha = 6$(− · − · −·), and $\alpha = 10$(· · ·) for the driven cavity problem.

In order to visualise the overall flow pattern inside the domain Ω we present in Figure 5 the velocity field at some selected interior points. The lengths of the vectors and of the arrows are proportional to the magnitude of the fluid velocity. Although not illustrated graphically, we wish to report that both the magnitude and the direction of the fluid vectors were observed to be similar to those obtained when solving both the direct and the inverse problem.

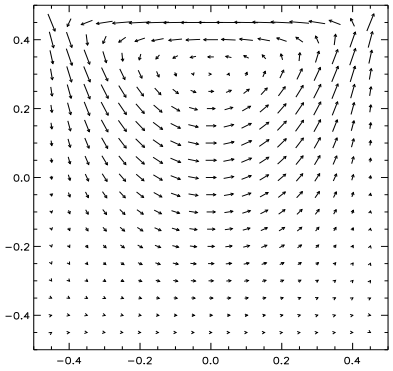

FIGURE 5. The velocity vectors at selected points inside the driven cavity obtained by solving the inverse problem with $\alpha = 0$ for $\Gamma_0 = \Gamma_1$ and $\Gamma^* = \Gamma_2$.

It is important to note that for the driven cavity problem with singularities, the solution is more sensitive to the location of the under-specified and over-specified boundaries, becoming less accurate at some points, especially on the under-specified boundary. Also these boundary errors propagate into the solution domain. However, the accuracy of the results improves by increasing the over-specified boundary.

5. **Conclusions**

In this paper the Stokes equations, subject to under-specified boundary conditions on the normal component of the fluid velocity v, but with additional pressure measurements available on another part of the boundary, have been studied. A boundary element discretisation has been applied to the resulting Laplace equations and the Tikhonov regularization method has been used to solve the resulting ill-conditioned system of linear algebraic equations. The technique has been validated for a typical benchmark test example and in a situation where no analytical solution is available in a square cavity. It has been shown that this regularized boundary element technique retrieves an accurate and stable numerical solution, both on the boundary and inside the solution domain, with respect to decreasing the amount of noise in the input

boundary data. Moreover, the numerical solutions converge for a reasonable number of boundary elements, about half the number of boundary elements used when solving the corresponding direct problem.

References

[1] Brebbia, C.A., Telles, J.C.F., and Wrobel, L.C., *Boundary Element Techniques: Theory and Applications in Engineering*, Springer-Verlag, Berlin, 1984.

[2] Brent, R.P., *Algorithm 488: A Gaussian Pseudo-Random Number Generator*, Commun. A. C. M., **17**(1974), 704-707.

[3] Curteanu, A., Ingham, D.B., Elliott, L., and Lesnic, D., *A Laplacian decomposition of the two-dimensional Stokes equation*, Fourth UK Conference on Boundary Integral Methods (Ed. S. Amini), Salford University Press, UK, 2003, 47-56.

[4] Hadamard, J., *Lectures on Cauchy Problem in Linear Partial Differential Equations*, Yale University Press, New Haven, 1923.

[5] Hansen, P.C., *Analysis of discrete ill-posed problems by means of the L-curve*, SIAM Rev., **34**(1992), 561-580.

[6] Mera, N.S., Elliott, L., Ingham, D.B., and Lesnic, D., *A comparison of boundary element method formulations for steady state anisotropic heat conduction problems*, Eng. Anal. Boundary Elem., **25**(2001), 115-128.

[7] Tikhonov, A.N., and Arsenin, V.Y., *Solutions of Ill-Posed Problems*, Winston-Wiley, Washington D.C, 1977.

[8] Zeb, A., Elliott, L., Ingham, D.B., and Lesnic, D., *Boundary element two-dimensional solution of an inverse Stokes problem*, Eng. Anal. Boundary Elem., **24**(2000), 75-88.

Department of Applied Mathematics, University of Leeds,
Leeds LS2 9JT, UK
E-mail address: amt6dbi@maths.leeds.ac.uk